

Auto-Focusing UWB Radar Imaging for Moving Human Target using Revised Range Point Migration

Takuya Sakamoto^{*†}, Toru Sato[†], Pascal Aubry^{*}, and Alexander Yarovoy^{*},

^{*}Delft University of Technology
Mekelweg 4, 2628CD Delft, the Netherlands
Email: T.Sakamoto@tudelft.nl

[†]Graduate School of Informatics, Kyoto University
Yoshida-Honmachi, Sakyo-ku, 606-8501 Kyoto, Japan

Abstract—We propose an ultra-wideband radar imaging algorithm that can be applied to moving targets with unknown speeds. The proposed method compensates for the motion of a human body to automatically generate focused images. The speed of the target is estimated using the image blurriness of the target’s head. In the estimation of speeds, we use the revised range point migration, which is known to be a fast radar imaging algorithm. Measurement results showed that the proposed method generates high-quality images for moving targets. A mannequin and a handgun were assumed as targets, of which both were clearly imaged, indicating the applicability of the proposed method to security systems.

Index Terms—radar imaging, head size, target motion, revised range point migration

I. INTRODUCTION

The well-known advantages of radar imaging sensors over optical ones for security and safety applications are radar capabilities to penetrate into different media and provide range and Doppler information of targets in addition to target images [1]. However, many conventional ultra wideband (UWB) imaging systems assume that a target remains static during measurements [2]-[7]. This assumption restricts the application of such systems. Furthermore, some of these systems use mechanically scanning array antennas to avoid costly large-scale array antennas. For these systems, neglecting target motion during measurements results in blurred images. Development of an auto-focusing imaging algorithm, which can compensate for target movement, would solve the bottleneck mentioned above resulting in extension of the UWB scanner applicability area and improve image quality.

Our previous study [8] proposed a target speed estimation algorithm for relatively small targets using the image sharpness metric. However, the method cannot be applied to large targets with numerous scattering centers such as human bodies, because an image obtained by correctly compensating for target motion is not always well-focused whereas wrongly-assumed motion can erroneously focus the target image.

In this paper, we propose an improved algorithm for estimating target speed using the blurriness of images of human bodies, exploiting the fact that human heads have relatively small individual differences. To demonstrate its performance, our method was applied to measurement data taken from a

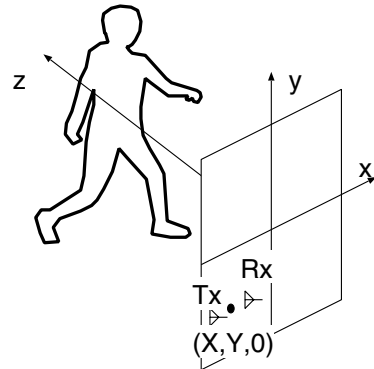


Fig. 1. System setup with antennas scanning from the x - y plane.

mannequin. We also applied the proposed method to a moving mannequin with a weapon to investigate its applicability in a security systems to detect weapons.

II. SYSTEM MODEL

The measurement system consists of a transmitter and a receiver positioned in the $z = 0$ plane in the direction of x at a fixed separation $2d$. The midpoint between the transmitter and receiver is labeled $(X, Y, 0)$, which means the transmitting and receiving antennas are located at $(X - d, Y, 0)$ and $(X + d, Y, 0)$, respectively. With the transmitter-receiver pair scanning at discrete intervals across a region of the $z = 0$ plane, UWB pulses are transmitted and pulse echoes are received. Figure 1 shows the system setup assumed in this paper.

The received signals contain not only echoes from the target but also a coupling signal propagating directly from the transmitter to the receiver. To eliminate this coupling signal, the background signal, measured without target prior to actual measurements, is subtracted from the received signal. Given the antennae midpoint $(X, Y, 0)$, the signal received is labeled $s(X, Y, Z)$, where $Z = ct/2$. Here, c is the speed of the electromagnetic wave and t is the time interval between transmission and reception.

III. BISTATIC INVERSE SCATTERING TRANSFORM

We developed a fast imaging algorithm using the bistatic inverse boundary transform (bistatic-IBST), which is a reversible transform between radar signals and radar images [9]. The first step in imaging using the bistatic-IBST is the extraction of signal peaks, which satisfy

$$\frac{\partial}{\partial Z}s(X, Y, Z) = 0, \quad (1)$$

$$|s(X, Y, Z)| > T_s, \quad (2)$$

where T_s is a constant threshold introduced to suppress noise. These peaks are indexed as (X_i, Y_i, Z_i) for $(i = 1, 2, \dots, N)$. The corresponding amplitudes of these peaks are denoted $s_i = s(X_i, Y_i, Z_i)$.

For a simple target shape, these points are easily connected sequentially to form multiple curved surfaces $Z(X, Y)$. This function, called a quasi-wavefront, is used in imaging with the bistatic inverse boundary scattering transform (IBST)

$$x = X - \frac{2Z^3 Z_X}{Z^2 - d^2 + \sqrt{(Z^2 - d^2)^2 + 4d^2 Z^2 Z_X^2}}, \quad (3)$$

$$y = Y + Z_Y \{d^2(x - X)^2 - Z^4\} / Z^3, \quad (4)$$

$$z = \sqrt{Z^2 - d^2 - (y - Y)^2 - \frac{(Z^2 - d^2)(x - X)^2}{Z^2}}, \quad (5)$$

where for simplicity $Z_X = \partial Z / \partial X$ and $Z_Y = \partial Z / \partial Y$.

Because of these derivative components, Z_X and Z_Y , the bistatic-IBST is, however, quite sensitive to noise. To obtain these derivatives, peaks need to be correctly connected when forming the curved surfaces. As this is not an easy task for complex-shaped targets such as human bodies, we need to introduce another method that can estimate stable derivatives. This is done in the next section.

IV. IMAGING USING REVISED RANGE POINT MIGRATION

To obtain stable derivatives Z_X and Z_Y , we introduced the revised range point migration (RRPM) method [10], which is known to be fast and robust even for complicated shapes in a noisy scenario.

The RRPM method estimates a derivative $Z_X = \tan(\hat{\theta}_i)$, where $\hat{\theta}_i$ is calculated as

$$\hat{\theta}_i = \frac{\sum_{j \neq i, Y_j = Y_i} w_{i,j} \tan^{-1} \left(\frac{Z_i - Z_j}{X_i - X_j} \right)}{\sum_{j \neq i, Y_j = Y_i} w_{i,j}}. \quad (6)$$

The weighting coefficient in Eq. (6) is defined as

$$w_{i,j} = |s_i s_j| \exp \left(-\frac{(X_i - X_j)^2}{\sigma_X^2} - \frac{(Z_i - Z_j)^2}{\sigma_Z^2} \right), \quad (7)$$

where σ_X and σ_Z are the scaling factors of the Gaussian function. The weight $w_{i,j}$ has a large value if the i -th and j -th peaks are close to each other in terms of the target range and antenna position. This weight determines the contributing strength of the j -th signal peak in calculating the derivative at the i -th peak. In a similar way, we can estimate Z_Y . Finally, these derivatives are substituted into Eqs. (3), (4), and (5), to obtain the target images. The combination of the RRPM

TABLE I
STATISTICAL DATA FOR PHYSICAL SIZES OF HUMANS

	average	5th percentile	95th percentile
waist circumf. [11]	90.2 cm	73.3 cm	118.4 cm
head breadth [12]	15.2 cm	14.3 cm	16.11 cm

method and the bistatic-IBST is known to be computationally fast; the study [10] showed the RRPM method was 170 times faster than the conventional diffraction stack migration under similar conditions.

V. HUMAN HEAD SIZE AND IMAGE FOCUSING

In our previous study, we proposed a target speed estimation method using the sharpness metric of radar images [8]. The method assumes that the target is relatively small and the image is best-focused when the assumed speed is correct. However, human bodies are relatively large and their individual differences are not negligible.

The width between the 5th and 95th percentiles of the waist circumference of males between 20 and 29 years old is 50% of the average [11], whereas the same value of the head breadth of males is only 12% [12]. These statistical values are shown in Table I. Because the individual difference is minimal, it is judicious to use images of the head to evaluate the sharpness of an image.

First, we estimate the head position of an image $I(x, y)$ by taking the largest peak of the vertical profile of the RRPM image as

$$y_h = \arg \max_y p_h(y), \quad (8)$$

$$\text{subject to } dp_h(y)/dy = 0, \quad (9)$$

$$|p_h(y)| > p_T, \quad (10)$$

where

$$p_h(y) = \int I(x, y) dx \quad (11)$$

is the vertical profile of the image, and p_T is a threshold used to avoid extracting artifacts. Although $I(x, y)$ can be any image, we use the image produced by the RRPM method assuming a stationary target.

Next, the image sharpness is evaluated using $I_h(x) = I(x, y_h)$. The peak point for the head is estimated as

$$x_p = \arg \max_x I_h(x), \quad (12)$$

and the image blurriness b is then defined from the mean and central moments of I_h as

$$b = \sqrt{\frac{\int (x - x_p)^2 I_h(x - x_p) dx}{\int I_h(x - x_p) dx}}. \quad (13)$$

We use the fast RRPM method for calculating the blurriness of these images because the imaging process is repeated for various assumed speeds; this process can be time consuming if conventional slow methods are used.



Fig. 2. Photo of metal-coated mannequin on a moving platform used for our measurement.

Once the target speed is estimated, we apply the diffraction stack migration method to produce three-dimensional (3-D) images. In the following sections, 3-D radar images are shown in the form of a 2-D energy projection onto the x - y plane, or a 3-D surface rendering of the image.

VI. APPLICATION TO MEASUREMENT

A. Measurement and Processing Setup

We applied our proposed method to measurement data obtained from a metal-coated mannequin on a moving platform (see Fig. 2). The mannequin moves along a straight line in the $-z$ direction as in Fig. 1.

We employed an Agilent PNA E8364B to sweep frequencies from 5.0 to 25.0 GHz with 251 sampling points. The distance between the transmitting and receiving antennas was 5.5 cm. The antennas scanned at 1.0 cm intervals over an area 75.0 cm \times 75.0 cm in the x - y plane. Hence the total number of measuring points is $76 \times 76 = 5776$. While the antennas scanned from left to right, the target moved towards the antennas a distance of 38.0 cm, corresponding to a target speed of 1.0 m/s, assuming a total measurement time of 0.38 s.

The RRPM method extracts 15 peaks for each antenna position. We set $\sigma_X = \sigma_Y = 0.8\text{cm}$, $\sigma_Z = 0.3\text{cm}$ and $\sigma_\theta = \pi/100$. The i -th target image point (x_i, y_i, z_i) is weighted with amplitude $|s_i|$ to generate an image. We set $p_T = 0.1$ for a normalized vertical profile, i. e. $\max p_h(y) = 1$.

B. Application to Mannequin Measurements

Figure 3 shows four images produced by the RRPM method assuming various target speeds. We see that the lower left image, corresponding to the correct speed 1.0 m/s, is the best-focused of the four. This property of the images is exploited to estimate the target speed in our proposed method.

The first step of the proposed method is the estimation of the head position y_h using the vertical profile $p_h(y)$ of the image $I(x, y)$ generated by the RRPM method assuming a zero speed. The image of $I(x, y)$ and its vertical profile $p_h(y)$ are shown in Fig. 4. The head position was estimated as $y_h = 13\text{cm}$ indicated as a dashed line in red in the figure.

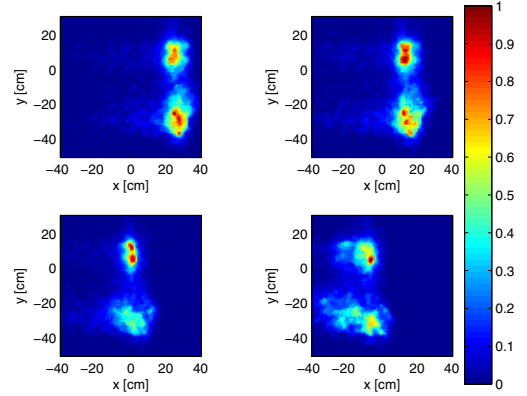


Fig. 3. Images obtained with the RRPM method for various assumed speeds 0 m/s (upper left), 0.5 m/s (upper right), 1.0 m/s (lower left), and 1.5 m/s (lower right) for an actual speed of 1.0 m/s.

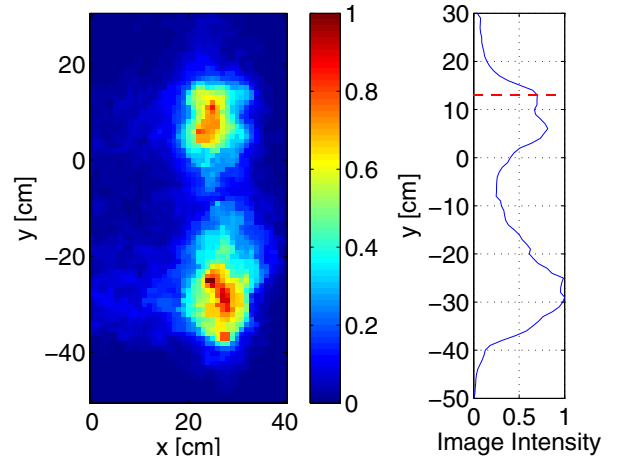


Fig. 4. Vertical profile (right) of the radar image (left) to determine head height; detected head height ($y_h = 13\text{cm}$) is shown as a red dashed line.

Using the estimated head position, we can now calculate the image blurriness defined in Eq. (13). Figure 5 shows the image blurriness b for different assumed speeds; its minimum is at 1.12 m/s whereas the actual speed is 1.0 m/s, corresponding to a 12% relative error. The radar image assuming the actual and estimated target speeds of 1.0 m/s and 1.12 m/s are shown in Fig. 6. The figure clearly shows an accurate image of the mannequin. This result shows that the estimation accuracy of the target speed is sufficiently high for imaging a human body.

Figure 7 shows the 3-D surface of the image for the estimated target speed, which corresponds to the right image of Fig. 6. This 3-D image also clearly depicts the head and chest part of the target, demonstrating the effectiveness of the proposed method.

C. Application to Measurement for a Mannequin with a Weapon

We applied the method to analyze measurement data obtained for a mannequin with a handgun against the chest (see

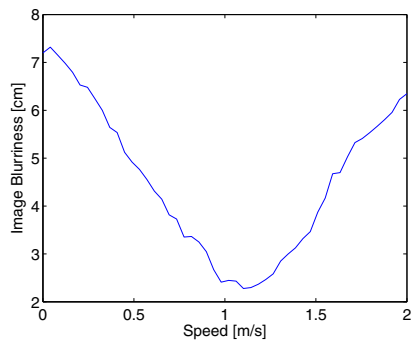


Fig. 5. Blurriness of the head image for various assumed speeds (actual speed: 1.0 m/s, estimated speed: 1.12 m/s).

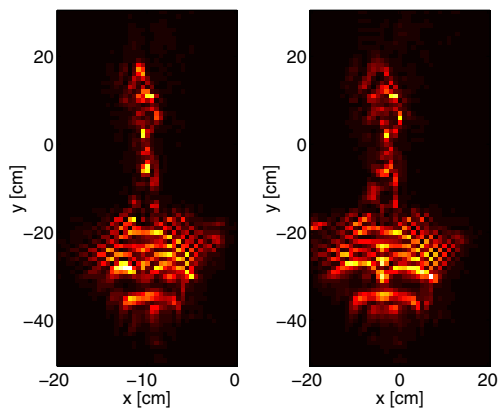


Fig. 6. Target images assuming actual speed (1.0 m/s, left) and estimated speed (1.12 m/s, right).

Fig. 8). The handgun is hung with a thin string so as not to affect measurements. Considering that the used frequency band allows penetration through clothes, this scenario simulates a weapon concealed under a jacket worn by a person.

Figure 9 shows the blurriness b of the estimated head image for the mannequin with a handgun. The blurriness is minimum when the assumed speed is 1.02 m/s, giving 2% relative error. Figure 10 shows the 3-D image generated using the estimated target speed for the mannequin with handgun. The shape of the handgun is clearly imaged in this figure, gives a promise to extend applicability area of the proposed method to the detection of concealed weapons from cooperative targets (humans, who can stay still while being scanned) to non-cooperative targets (scanning while humans are moving towards the gate).

In this paper, we have applied the proposed method to a mannequin instead of an actual human. To apply the method to an actual person, we need to cope with the blurriness caused by limb motion, which is an important future task.

VII. CONCLUSION

We proposed an auto-focusing imaging algorithm for UWB radar that is applicable to moving targets with unknown speeds. The proposed method estimates the speed of a human

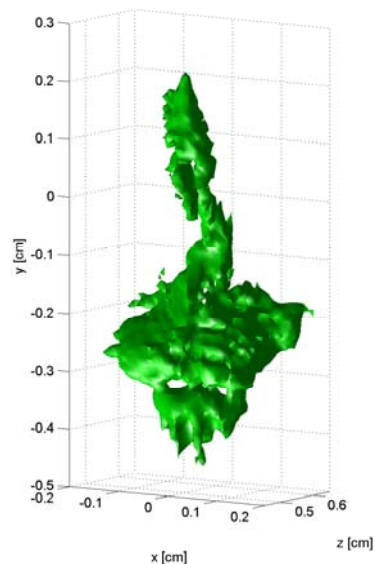


Fig. 7. Three-dimensional surface image of a mannequin using the estimated speed of 1.12 m/s.



Fig. 8. A mannequin with a handgun on its chest used for our measurement.

target using the blurriness of the head image generated by the RRPM method, which is known as a fast imaging algorithm. This method first estimates the head position. Assuming various target speeds, multiple radar images are generated using the RRPM method. For each image, the blurriness of the head is evaluated to estimate the actual speed. Finally, to mitigate the blurriness, the estimated speed is then used to obtain a focused image. We applied the proposed method to measurement data for two scenarios of a moving mannequin with and without a handgun; the estimated target speeds produced relative errors of 12 % and 2%, respectively. The results showed that the accuracy of the proposed method was sufficient in practice for producing high-quality images of a human body. In particular, the mannequin with handgun was imaged clearly enough for the handgun to be identified in the image. This result suggests that the proposed method is

promising in its applicability to security systems for detecting concealed weapons.

ACKNOWLEDGMENT

This study was supported in part by the Japan Society for the Promotion of Science (JSPS) Postdoctoral Fellowships for Research Abroad (High-resolution imaging for human bodies with UWB radar using multipath echoes).

REFERENCES

- [1] A. G. Yarovoy, T. G. Savelyev, P. J. Aubry, P. E. Lys, L. P. Ligthart, "UWB array-based sensor for near-field imaging," *IEEE Transactions on Microwave Theory and Techniques*, vol. 55, no. 6, part 2, pp. 1288–1295, June 2007.
- [2] X. Zhuge, A. G. Yarovoy, T. Savelyev, L. Ligthart, "Modified Kirchhoff migration for UWB MIMO array-based radar imaging" *IEEE Transactions on Geoscience and Remote Sensing*, vol. 48, no. 6, pp. 2692–2703, 2010.
- [3] X. Zhuge, and A. Yarovoy, "A sparse aperture MIMO-SAR based UWB imaging system for concealed weapon detection," *IEEE Transactions on Geoscience and Remote Sensing*, vol. 49 no. 1, pp. 509–518, 2011.
- [4] Y. Wang, Y. Yang, A. E. Fathy, "Experimental assessment of the cross coupling and polarization effects on ultra-wide band see-through-wall imaging reconstruction," *IEEE MTT-S International Microwave Symposium Digest*, pp. 9–12, June 2009.
- [5] A. Nelander, "Switched array concepts for 3-D radar imaging," *Proc. 2010 IEEE Radar Conference*, pp. 1019–1024, 2010.
- [6] T. Counts, A. C. Gurbuz, W. R. Scott Jr., J. H. McClellan, and K. Kim, "Multistatic ground-penetrating radar experiments," *IEEE Trans. Geoscience and Remote Sensing*, vol. 45, no. 8, pp. 2544–2553, Aug. 2007.
- [7] Y. Yang and A. E. Fathy, "Development and implementation of a real-time see-through-wall radar system based on FPGA," *IEEE Trans. Geoscience and Remote Sensing*, vol. 47, no. 5, pp. 1270–1280, May 2009.
- [8] T. Sakamoto, T. Sato, P. Aubry, and A. Yarovoy, "Target Speed Estimation Using Revised Range Point Migration for Ultra Wideband Radar Imaging," *Proc. European Conference on Antennas and Propagation 2013*, April 2013.
- [9] S. Kidera, Y. Kani, T. Sakamoto and T. Sato, "A fast and high-resolution 3-D imaging algorithm with linear array antennas for UWB pulse radars," *IEICE Trans. on Communications*, vol. E91-B, no. 8, pp. 2683–2691, 2008.
- [10] T. Sakamoto, T. G. Savelyev, P. J. Aubry and A. G. Yarovoy, "Revised Range Point Migration Method for Rapid 3-D Imaging with UWB Radar," *Proc. 2012 IEEE International Symposium on Antennas and Propagation and USNC-URSI National Radio Science Meeting*, 508.2, July 2012.
- [11] U.S. Department of Health and Human Services, *Anthropometric Reference Data for Children and Adults: United States, 2007–2010*, Oct. 2012.
- [12] United States Army Missile Command, *Human engineering design data digest*, CreateSpace Independent Publishing Platform, 1984.

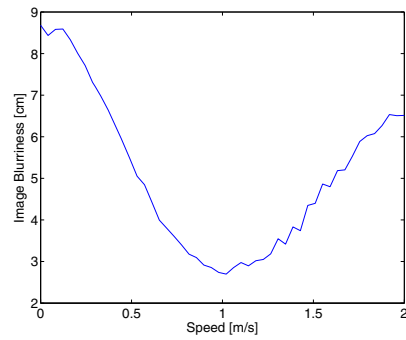


Fig. 9. Blurriness of the head image for a mannequin with a handgun (actual speed: 1.0 m/s, estimated speed: 1.02 m/s).

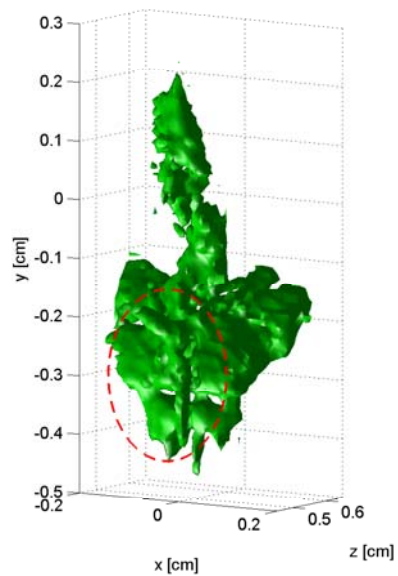


Fig. 10. Three-dimensional surface image of a mannequin with a handgun using the estimated speed of 1.02 m/s. The handgun is encircled in red.